NUMERICAL EXAMPLES

1. Model

Let Ω be a convex polygon in $\mathbf{R}^2$ with boundary Γ. Let $D \subseteq \Omega$ be a domain in $\mathbf{R}^2$ with Lipschitz boundary.

Let $B(x_0, r) = \{x \in \mathbf{R}^2 : |x - x_0| < r\}$. Let $B_j = B(\bar{x}_j, \delta), 1 \leq j \leq N$, be mutually disjoint subdomains inside Ω that are occupied by the wells. Set $\Gamma_j = \partial B_j$ and $\Omega_\delta = \Omega \backslash (\cup_{j=1}^N \bar{B}_j)$. We consider the following problem

$$-\mathrm{div}\,(K(x)\nabla u_\delta) = 0 \quad \text{in } \Omega_\delta, \tag{1.1}$$

$$u_\delta|_{\Gamma_j} = \mathrm{const}\,, \quad -\int_{\Gamma_j} K\frac{\partial u_\delta}{\partial \nu} ds = \mathrm{q}_j \quad \text{for } j \in I_M, \tag{1.2}$$

$$u_\delta|_{\Gamma_j} = \alpha_j \quad \text{for } j \in I_D, \quad u_\delta|_\Gamma = 0. \tag{1.3}$$

Here I_D, I_M are index sets such that $I_D \cup I_M = \{1, 2, \cdots, N\}$, α_j for $j \in I_D$ and q_i for $i \in I_M$ are known constants. We imposed the following conditions on the coefficient $K(x)$:

(H1) $K \in C^{0,1}(\bar{\Omega})$, there exist constants $\lambda, \Lambda > 0$ such that $\lambda \leq K(x) \leq \lambda^{-1}$ and $|K(x) - K(y)| \leq \Lambda|x - y|$ for any $x, y \in \bar{\Omega}$. As we are interested in highly variable coefficients, without lost of generality, we assume $\Lambda \geq 1$.

We will consider the following approximation of the problem (1.1)-(1.3): Find u and the constants $\{\mathrm{q}_i\}_{i \in I_D}$, such that

$$-\mathrm{div}\,(K(x)\nabla u) = \sum_{j=1}^N \mathrm{q}_j \delta_{\bar{x}_j} \quad \text{in } \Omega, \tag{1.4}$$

$$-\frac{\mathrm{q}_i}{2\pi K_i}\ln\delta + \sum_{j \neq i} \mathrm{q}_j \phi_j(\bar{x}_i) + U(\bar{x}_i) = \alpha_i \quad \text{for } i \in I_D, \tag{1.5}$$

$$u|_\Gamma = 0. \tag{1.6}$$

Here $\delta_{\bar{x}_j}$ is the Dirac measure at $\bar{x}_j$, $K_j = K(\bar{x}_j)$, $\phi_j(x) = -\frac{1}{2\pi K_j}\ln|x - \bar{x}_j|$, and $U = u - \sum_{j=1}^N \mathrm{q}_j \phi_j$. The relation (1.5) can be viewed as an approximation of the boundary condition $u|_{\Gamma_i} = \alpha_i$ for $i \in I_D$.

We have the following theorem.

Theorem 1.1. *Let the assumption (H1) be satisfied. Let u_δ and u be the solutions of* (1.1)-(1.3) *and* (1.4)-(1.6)*, respectively. Then there exists a constant C*

independent of δ, q_j *and* Λ *such that*

$$\max_{x\in\bar{\Omega}_\delta}|u-u_\delta| \le C\Lambda(1+\ln\Lambda)^{1/2}\Big(\sum_{j=1}^{N}|\mathrm{q}_j|\Big)\delta|\ln\delta|. \tag{1.7}$$

2. Numerical results

We start this section by summarizing the algorithm proposed in this chapter for solving the problem (1.4)-(1.6) which is a good approximation of the original problem (1.1)-(1.3) when the size of the wells is negligible.

Algorithm 1. Given the well bore pressure α_i for $i \in I_D$ and the well flow rate q_j for $j \in I_M$. The following procedure finds the approximate well bore pressure α_j^H for $j \in I_M$, the approximate well flow rate q_i^H for $i \in I_D$, and the approximate pressure $u_H = \zeta_H + \sum_{j=1}^N \mathrm{q}_j^H G_j^h$, where $\mathrm{q}_j^H = \mathrm{q}_j$ for $j \in I_M$.

- For $j = 1, \cdots, N$, compute the discrete Green function G_j^h on each subdomain Ω_j, i.e. $G_j^h \in V_h^0(\Omega_j)$ such that

$$\int_{\Omega_j} K(x)\nabla G_j^h \nabla v_h dx = v_h(\bar{x}_j) \quad \forall v_h \in V_h^0(\Omega_j). \tag{2.1}$$

  Here $V_h^0(\Omega_j) = V_h(\Omega_j) \cap H_0^1(\Omega_j)$, and $V_h(\Omega_j)$ is the standard conforming linear finite element space over the mesh $\mathcal{M}_h(\Omega_j)$ of Ω_j with the mesh size h resolving the scale of the permeability field $K(x)$. Compute the associate effective radius $\bar{r}_j$ from G_j^h according to the discussion in §6. Thus the approximate value of the Green function G_j on Γ_j is

$$\alpha_j^h = G_j^h(\bar{x}_j) - \frac{1}{2\pi K_j}\ln\frac{\delta}{\bar{r}_j}, \quad K_j = K(\bar{x}_j).$$

- Use the over-sampling multiscale finite element method to find $\zeta_H \in X_H^0$ and $\{\mathrm{q}_i^H\}_{i\in I_D}$ such that

$$\sum_{T\in\mathcal{M}_H}\int_T K(x)\nabla\zeta_H\nabla\chi_H dx = -\sum_{j=1}^{N}\mathrm{q}_j^H\int_{\Sigma_j} K\frac{\partial G_j^h}{\partial\nu}\hat{\chi}_H ds \quad \forall\chi_H \in X_H^0, \tag{2.2}$$

$$\mathrm{q}_i^H\alpha_i^h + \zeta_H(\bar{x}_i) = \alpha_i \quad \text{for } i \in I_D. \tag{2.3}$$

- Compute the approximate well bore pressure α_j^H for $j \in I_M$ through the relation

$$\alpha_j^H = \zeta_H(\bar{x}_j) + \mathrm{q}_j\alpha_j^h.$$

Now we present some numerical examples carried out for periodic local periodic and random log-normal permeability fields to demonstrate the accuracy and efficiency of our method. The computations are performed on the unit square

$\Omega = (0,1) \times (0,1)$. We consider two wells $B_j = B(\bar{x}_j, \delta)$ with $x_1 = (\frac{1}{4}, \frac{3}{4})$, $x_2 = (\frac{3}{4}, \frac{1}{4})$ and the radius $\delta = 10^{-5}$. We impose mixed boundary condition (1.2) that fixes the well flow rate q_j for both wells. Thus we have $I_D = \emptyset$ and the interested quantities are well bore pressure (WBP) on each well. In the computations we always take $\mathrm{q}_1 = -1$ and $\mathrm{q}_2 = 1$ which corresponds to the situation that the well B_1 is an extraction well and B_2 is an injection well.

The domain Ω_j is taken as the square centered at $\bar{x}_j$ with the length of the sides being $2H_j$ so that $H_j = \mathrm{dist}\,(\bar{x}_j, \partial\Omega_j)$. The discrete Green function G_j^h in (2.1) is computed on a uniform finite element mesh of size $h = H_j/512$.

A uniform $L \times L$ finite element mesh of Ω is constructed by first dividing the domain Ω into $L \times L$ subrectangles and then connecting the lower-left and the upper-right vertices of each subrectangle. The finite elements of the mesh is divided into two groups: the lower-right and upper-left elements. For each triangle T, an over-sampling element $S(T)$ is created according to whether T is a lower-right element or an upper-left element as shown in Figure 1. Here we assume that the permeability field is known outside the domain Ω when the over-sampling element $S(T)$ is extended outside Ω. This assumption is not a restriction for practical applications because the permeability is generated by geostatistical method based on the statistical characteristics which are usually known outside the interested domain.

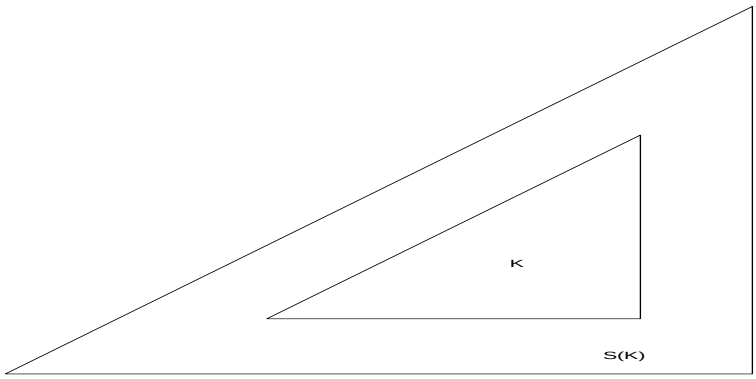

FIGURE 1. The element K and its over-sampling element $S(K)$: lower-right elements (left) and upper-left elements (right). The length of the horizontal and vertical edges of $S(K)$ is four times of the corresponding length of the edges of K.

For each triangle T, the over-sampling multiscale base functions on the over-sampling element $S(T)$ are computed on a uniform triangular mesh which divides

the horizontal and vertical edges of $S(T)$ into $4M$ subintervals, respectively. So the mesh size for solving the base functions is $1/LM$ in each space direction.

All the resultant linear algebraic system of equations is solved by the multigrid method.

Example 1. In this example we assume the coefficient is

$$K_\varepsilon(x) = \frac{1}{(2 + 1.5 \sin \frac{2\pi x}{\varepsilon})(2 + 1.5 \sin \frac{2\pi y}{\varepsilon})}.$$

The exact solution of the problem is unknown and so we compare the coarse grid solution obtained by Algorithm 1 with the well resolved solution on a uniform 2048×2048 mesh using the method introduced in §6 which can be easily extended to multi-well problems. This well resolved solution will be referred as "exact" solution in the following. For example, when $\varepsilon = 1/64 = 0.015625$, the "exact" well bore pressures are $\alpha_1 = -5.3884973$ in the first well and $\alpha_2 = 5.3884973$ in the second well.

The homogenized coefficient matrix K^* is known as $K^* = \frac{1}{\sqrt{7}}\mathrm{I}$, where I is the 2×2 identity matrix [**?**]. The standard homogenization method would be to approximate the original problem by

$$-\mathrm{div}\,(K^*(x)\nabla u^*) = \sum_{j=1}^{2} \mathrm{q}_j \delta_{\bar{x}_j} \quad \text{in } \Omega, \qquad u^*|_\Gamma = 0.$$

Table 2.1 shows the well bore pressures computed by solving above homogenized problem using the Peaceman method over uniform meshes. It clearly indicates that the standard homogenization method fails to provide good approximations in the vicinity of well singularities. This shows the importance to develop new upscaling methods for flow transport problems involving well singularities.

Neglecting the logarithm factors, the convergence rate of Algorithm 1 is $O(H + H^2/H_j^2 + \varepsilon/H + \sqrt{\varepsilon/H_j})$. In Table 2.2, we test the convergence of our method when ε/H is fixed to be 0.5. We see that the solution still converges as ε decreases. This shows that the constant in the ε/h term in the error estimate is small. We also observe that the convergence rate is better than $\sqrt{\varepsilon}$ when the resonant error term ε/H is not dominant. In Table 2.3, we show the errors for a fixed $\varepsilon = 1/64$. We observe that the errors increase as H decreases, indicating the existence of the error term ε/H in the error estimate. The resonant error is the strongest when $\varepsilon = H$. We remark that previous studies indicate that the cell resonance error is more visible for periodic coefficients, especially when ε/H is a rational number. But the cell resonance error is generically small for random coefficients. Table 2.4 shows the influence of the size H_j of local domain Ω_j to the overall convergence of the method. It indicates that in practical computations, the size of the local

L	Well No.	WBP	Relative error
32	1	-4.3624648	0.19041
64	1	-4.3626761	0.19037
128	1	-4.3627285	0.19036
32	2	4.3624648	0.19041
64	2	4.3626761	0.19037
128	2	4.3627285	0.19036

TABLE 2.1. Example 1: Results of the standard homogenization method, $\varepsilon = 1/64$.

L	ε	Well No.	WBP	Relative error	Rate
8	1/16	1	-5.6634649	0.54608E-02	
16	1/32	1	-5.5312112	0.22704E-02	1.2662
32	1/64	1	-5.3842752	0.78354E-03	1.5349
8	1/32	2	5.6615759	0.57925E-02	
16	1/32	2	5.5281669	0.28195E-02	1.0387
32	1/64	2	5.3802340	0.15335E-02	0.8786

TABLE 2.2. Example 1: Results of the Algorithm 1, $H_j = 1/8$, $M = 64$.

domain Ω_j need not be very large (two or three times of the size of the coarse mesh would be enough). Remember that smaller local domains Ω_j reduce the cost of computing the discrete Green functions. However, we emphasize that the discrete Green functions need only to be computed once which is a just small overhead of the overall computations. Actually, in Table 2.5 we find that when the local domain is small, it is not necessary to solve the local Green's function on much more fine grid, and we can solve it just by the cost of construction a multiscale finite element basis.

L	M	Well No.	WBP	Relative error	Rate
8	256	1	-5.3683706	0.37351E-02	
16	128	1	-5.3828001	0.10573E-02	1.8207
32	64	1	-5.3842752	0.78354E-03	0.4323
64	32	1	-5.3838442	0.86352E-03	-0.1402
8	256	2	5.3713129	0.31891E-02	
16	128	2	5.3825320	0.11070E-02	1.5256
32	64	2	5.3802340	0.15335E-02	-0.4702
64	32	2	5.3739254	0.27043E-02	-0.8184

TABLE 2.3. Example 1: Results of the Algorithm 1, $\varepsilon = 1/64$, $H_j = 1/8$.

Well No.	H_j	WBP	Relative error	Rate
1	H	-5.3133941	0.139377E-01	
1	2H	-5.3519482	0.678280E-02	1.0390
1	4H	-5.3700536	0.342279E-02	0.9867
2	H	5.3123314	0.141349E-01	
2	2H	5.3497078	0.719858E-02	0.9735
2	4H	5.3653456	0.429650E-02	0.7445

TABLE 2.4. Example 1: Influence of the size of the local domain Ω_j, $\varepsilon = 1/64, L = 64, M = 32$.

Example 2 In this example, we set

$$K_\varepsilon(x) = \frac{2 + p\sin(\frac{2\pi x}{\varepsilon})}{2 + p\sin(\frac{2\pi y}{\varepsilon})} + \frac{2 + p\sin(\frac{2\pi y}{\varepsilon})}{2 + p\sin(\frac{2\pi x}{\varepsilon})},$$

with $p = 1.8$ The homogenizatioin K^* of K_ε is a full 2×2 matrix. Tables 2.6-2.10 show that our method works very well.

Well No.	h	WBP	Relative error
1	$H_j/512$	-5.3133941	0.1394E-01
1	$H_j/128$	-5.3117237	0.1425E-01
1	$H_j/64$	-5.3086750	0.1481E-01
1	$H_j/32$	-5.3003683	0.1636E-01
1	$H_j/16$	-5.2771637	0.2066E-01
1	$H_j/8$	-5.2141346	0.3236E-01

TABLE 2.5. Example 1: Influence of the resolution for the local Green's function, $L = 64, M = 32$, $H_j = H$

L	ε	Well No.	WBP	Relative error	Rate
8	1/16	1	-0.8846656	0.4430E-02	
16	1/32	1	-0.8489153	0.2234E-02	1.0507
32	1/64	1	-0.8117082	0.1281E-02	0.8682
8	1/16	2	0.8835495	0.4849E-02	
16	1/32	2	0.8482490	0.2582E-02	0.9717
32	1/64	2	0.8112662	0.1598E-02	0.7579

TABLE 2.6. Example 2: Results of the Algorithm 1, $H_j = 1/8$, $M = 64$

Example 3 In this example, we consider a local periodic permeability case. we set

$$K_\varepsilon(x) = \frac{1+y}{2+p\sin(\frac{2\pi x}{\varepsilon})} + \frac{1+x}{2+p\sin(\frac{2\pi y}{\varepsilon})},$$

with $p = 1.8$ Tables 2.11-2.13 show the results.

Example 4. In this example, we test the performance of our method for a random log-normal permeability field. We generate the random field $K(x)$ on a uniform 1024×1024 mesh by using moving ellipse average technique [**?**] with the variance of the logarithm of the permeability $\sigma^2 = 1$, and the correlation lengths $l_x = l_y = 0.01$ in two space direction. Figure 2 shows a realization of the random permeability

L	M	Well No.	WBP	Relative error	Rate
8	256	1	-0.8102849	0.3032E-02	
16	128	1	-0.8117010	0.1290E-02	1.2331
32	64	1	-0.8117082	0.1281E-02	0.0100
64	32	1	-0.8109034	0.2271E-02	-0.8262
8	256	2	0.8103127	0.2771E-02	
16	128	2	0.8115042	0.1305E-02	1.0866
32	64	2	0.8112662	0.1598E-02	-0.2922
64	32	2	0.8101230	0.3005E-02	-0.9112

TABLE 2.7. Example 2: Results of the algorithm 1, $\varepsilon = 1/64,\ H_j = 1/8$

Well No.	H_j	WBP	Relative error	Rate
1	H	-0.7996270	0.1615E-01	
1	2H	-0.8053405	0.9116E-02	0.8247
1	4H	-0.8084997	0.5229E-02	0.8019
2	H	0.7992714	0.1636E-01	
2	2H	0.8049268	0.9399E-02	0.7995
2	4H	0.8079624	0.5664E-02	0.7308

TABLE 2.8. Example 2: Influence of the size of Ω_j, $\varepsilon = 1/64, L = 64, M = 32$

field. The "exact" well bore pressures computed by solving the problem (1.4)-(1.6) on the fine 1024×1024 mesh are $\alpha_1 = -1.7383199$ and $\alpha_2 = 3.0999852$.

Table 2.14 shows the results computed by using the Algorithm 1 on the coarse 64×64 mesh with the size of the local domains $H_1 = H_2 = H$. The mesh size for solving the over-sampling base functions is $1/1024$. It clearly shows that the WBP by our method on the coarse 64×64 mesh is a very good approximation of the "exact" WBP on the fine 1024×1024 mesh. In Figure 3 we show the contour plots of the pressure field computed by Algorithm 1 on the 64×64 mesh. As a comparison, we show in Figure 4 the contour plots of the averaged "exact" pressure

Well No.	h	WBP	Relative error
1	$H_j/512$	-0.7996270	0.1615E-01
1	$H_j/128$	-0.7996541	-0.1607E-01
1	$H_j/64$	-0.7996735	-0.1605E-01
1	$H_j/32$	-0.7996491	-0.1608E-01
1	$H_j/16$	-0.7993088	-0.1649E-01
1	$H_j/8$	-0.7956049	-0.2105E-01

TABLE 2.9. Example 2: Influence of the resolution for the local Green's function, $L = 64, M = 32$, $H_j = H$

Well No.	h	WBP	Relative error
1	$H_j/512$	0.7992714	0.1636E-01
1	$H_j/128$	0.7993034	-0.1628E-01
1	$H_j/64$	0.7993268	-0.1625E-01
1	$H_j/32$	0.7993096	-0.1627E-01
1	$H_j/16$	0.7989799	-0.1668E-01
1	$H_j/8$	0.7952739	-0.2124E-01

TABLE 2.10. Example 2: Influence of the resolution for the local Green's function, $L = 64, M = 32$,$H_j = 4H$

which is obtained by averaging the "exact" pressure field on the 1024×1024 mesh to the coarse 64×64 mesh. We observe from these figures and Table 2.14 that our method provides good approximation of the well bore pressure as well as the large scale structure of the "exact" solutions for random log-normal permeability field.

Example 5 In this example, we test the performance of our method for another random log-normal permeability field. We also generate the random field $K(x)$ on a uniform 1024×1024 mesh but with the variance of the logarithm of the permeability $\sigma^2 = 1$, and the correlation lengths $l_x = 0.01, l_y = 0.1$ in two space direction. Figure 5 shows a realization of the random permeability field. The

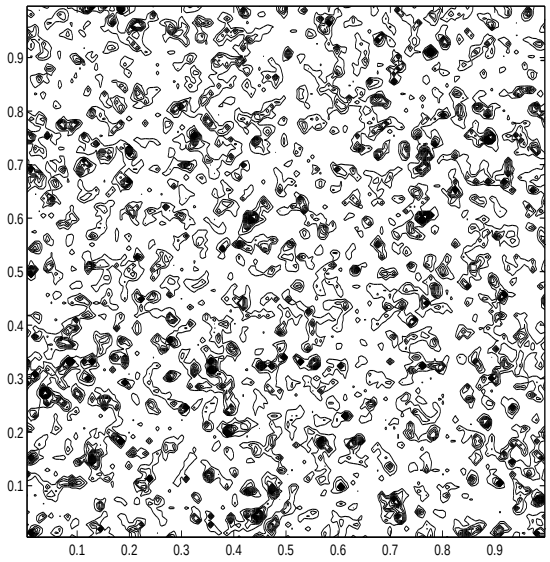

FIGURE 2. Example 4: The random log-normal permeability field $K(x)$. The ratio of maximum to minimum is 4.15443E+03.

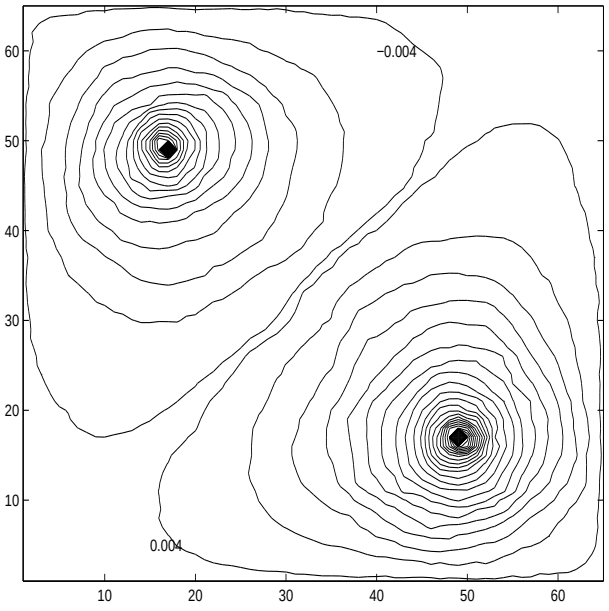

FIGURE 3. Example 4: Contour plots of the pressure field on 64×64 mesh by using Algorithm 1.

L	ε	Well No.	WBP	Relative error	Rate
8	1/16	1	-0.9068712	0.4894E-02	
16	1/32	1	-0.8757308	0.1868E-02	1.3893
32	1/64	1	-0.8423513	0.8326E-03	1.1660
8	1/16	2	0.9055985	0.6291E-02	
16	1/32	2	0.8745462	0.3219E-02	0.9669
32	1/64	2	0.8410716	0.2351E-02	0.4534

TABLE 2.11. Example 3: Results of the Algorithm 1, $H_j = 1/8,\ M = 64$

L	M	Well No.	WBP	Relative error	Rate
16	128	1	-0.8421446	0.1078E-02	
32	64	1	-0.8423513	0.8326E-03	0.3723
64	32	1	-0.8420159	0.1230E-02	-0.5634
16	128	2	0.8416962	0.1610E-02	
32	64	2	0.8410716	0.2351E-02	-0.5462
64	32	2	0.8392265	0.4539E-02	-0.9494

TABLE 2.12. Example 3: Results of the Algorithm 1, $\varepsilon = 1/64,\ H_j = 1/8$

'exact' well bore pressures computed by solving the problem (1.4)-(1.6) on the fine 1024×1024 mesh are $\alpha_1 = -1.1032187, \alpha_2 = 1.0118474$.

Table 2.15 shows the results computed by using the Algorithm 1 on the coarse 64×64 mesh with the size of the local domains $H_1 = H_2 = H$. The mesh size for solving the over-sampling base functions is $1/1024$. Figures 6-7 present the contour plots of the pressure fields of approximate and 'exact' solution respectively.

Appendix: The algorithm of moving ellipse method

To generate a 2-d log-normal random permeability field on a $nx * ny$ mesh on the unit square, with prescribe expectation E, variance σ and correlation length l_x, l_y at each direction, the algorithm is as follows

Well No.	H_j	WBP	Relative error	Rate
1	H	-0.9075988	0.7656E-01	
1	2H	-0.8956691	0.6241E-01	0.2948
1	4H	-0.8805615	0.4449E-01	0.4883
2	H	0.9018898	0.6979E-01	
2	2H	0.8906854	0.5650E-01	0.3048
2	4H	0.8763498	0.3949E-01	0.5166

TABLE 2.13. Example 3: Influence of the size of Ω_j, $\varepsilon = 1/64, L = 64, M = 32$

Well No.	WBP	Relative error
1	-1.7195261	0.1081E-01
2	3.1173632	0.5606E-02

TABLE 2.14. Example 4: Results of the Algorithm 1 in the case of random log-normal field with $\sigma^2 = 1$ and $l_x = l_y = 0.01$.

Well No.	Radius	'Exact' WBP	WBP	Relative error
1	1.E-05	-1.1032187	-1.1000738	0.2851E-02
1	1.E-04	-0.8749645	-0.8718196	0.3594E-02
1	1.E-03	-0.6467104	-0.6435655	0.4863E-02
2	1.E-05	1.0118474	1.0058803	0.5897E-02
2	1.E-04	0.8063361	0.8003690	0.7400E-02
2	1.E-03	0.6008248	0.5948576	0.9932E-02

TABLE 2.15. Example 5: Results of the Algorithm 1 in the case of random log-normal field with $\sigma^2 = 1$ and $l_x = 0.01$, $l_y = 0.1$.

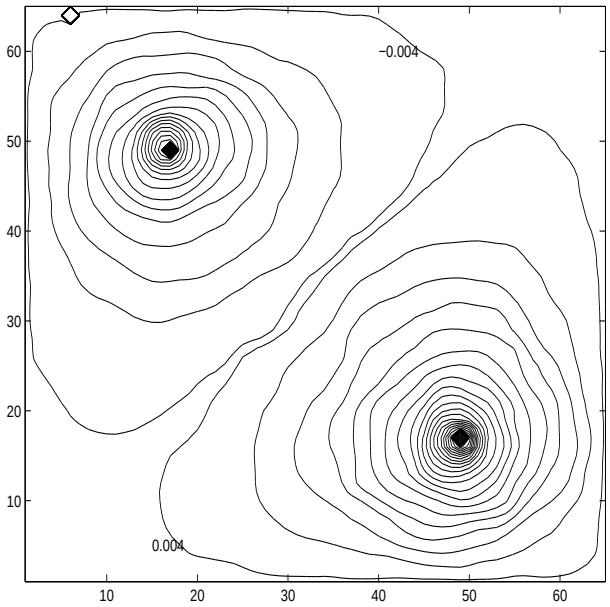

FIGURE 4. Example 4: Contour plots of the averaged "exact" pressure field on the 64×64 mesh

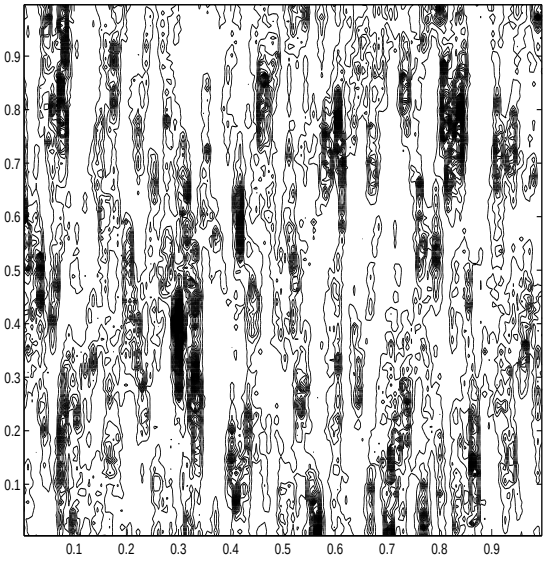

FIGURE 5. Example 5: The random log-normal permeability field $K(x)$, The ratio of maximum to minimum is 3.6710E+03

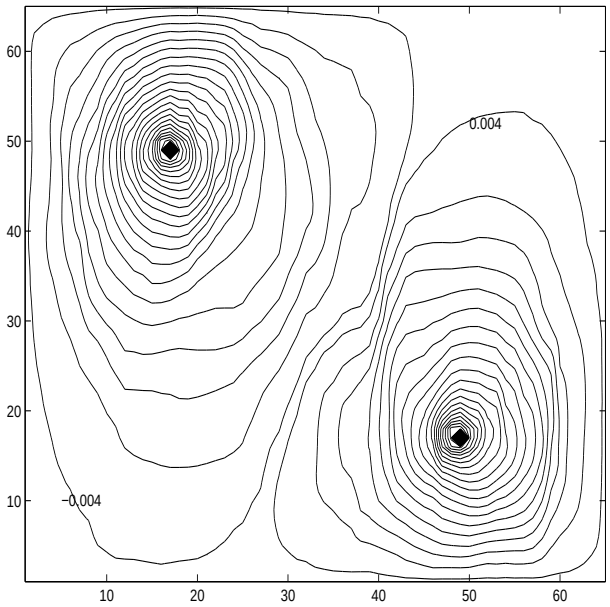

FIGURE 6. Example 5: Contour plots of the pressure field on 64×64 mesh by using Algorithm 1.

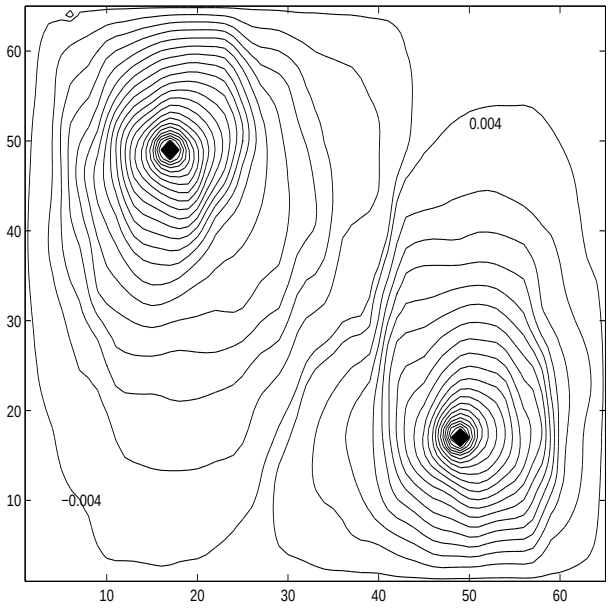

FIGURE 7. Example 5: contour plots of the averaged 'exact' pressure field on 64×64 mesh.

(1) Using 1-d normal random number generator to assign each mesh block a random number.
(2) For each mesh block, average the random numbers over all the blocks covered by the ellipse centered at the center of this block with l_x and l_y as its two axles, and then assign the average value to the block.
(3) Rescale the 2-d random field to satisfy the given expectation E and variance σ.
(4) Apply the function 'exp' to get the final log-normal field.